Distributed Koopman-Based Control of Improved Swing Equation

Vladimir Toro, Duvan Tellez-Castro, Eduardo Mojica-Nava, Naly Rakoto-Ravalontsalama

Available online at www.sciencedirect.com

ScienceDirect

IFAC Papers Online CONFERENCE PAPER ARCHIVE

IFAC PapersOnLine 55-13 (2022) 97–102

Distributed Koopman-Based Control of Improved Swing Equation

Vladimir Toro * **Duvan Tellez-Castro** * **Eduardo Mojica-Nava** *
Naly Rakoto-Ravalontsalama **

* *Universidad Nacional de Colombia, Bogotá, 111321 Colombia (e-mail: bwtorot@unal.edu.co, eamojican@unal.edu.co, datellezc@unal.edu.co).*

** *IMT Atlantique Bretagne-Pays de la Loire, 44307 France (e-mail: naly.rakoto@imt-atlantique.fr)*

Abstract: This paper presents a data-driven control for a set of synchronous generators based on the improved swing equation model by using the Koopman operator. First, the nonlinear dynamic of the generators is represented by a linear model in lifted space using extended dynamic mode decomposition (EDMD). Then, a linear predictor is built and used for the design of a model predictive control following three strategies: decentralized, non-cooperative, and cooperative. The Koopman representation of the generator is used to carry out an analysis, determining its eigenvalues. Several interconnected generators are controlled showing the performance of the interconnected system including voltage faults.

Keywords: Swing equation, model predictive control, Koopman operator, synchronous generator, distributed control.

1. INTRODUCTION

The reduction in the prices of renewable and diesel-based sources has boosted the design and implementation of small electrical systems. These elements are the foundation for building the microgrid, which is a cyber-physical system that gathers generators, loads, and storage devices capable of supplying demand even if it is disconnected from the utility network. When the microgrid works in islanded mode, the conditions for power-quality and availability are guaranteed by the set of sources. Several MGs are inverter-based, causing the MG to have a low-inertia, which is critical when abrupt load changes occur, and provoking changes in the frequency of the microgrid, degrading the power-quality, and compromising the stability of the system. In MGs with synchronous machines and inverters, the inertia is dominated by synchronous generators because of the fast response of inverters Tamrakar et al. (2020), this makes the study of stability in synchronous generators a paramount problem.

There are several control strategies for synchronous machines and microgrids; most of them are based on the swing equation model that relates to electrical and mechanical powers Bouzid et al. (2015). A linear swing equation is used to simplify control design; however, this reduces the accuracy of the control strategy. Zhou and Ohsawa (2008) presents an improved swing nonlinear equation which is used to analyze equilibrium points for a generator connected to an infinite bus. Monshizadeh et al. (2016) uses the nonlinear model of the swing equation to analyze the domain of attraction when the synchronous generator is connected to a constant load and to an infinite bus. In addition, stability is proved by using a Lyapunov function. Caliskan and Tabuada (2015) shows some problems of using swing equation and prove stability even with small oscillations. Finally, Vaidya et al. (1999) shows the existence of chaotic behavior in a three generator system using swing equation.

The nonlinear model has some limitations when it is used in traditional control techniques. The behavior of the system might be unpredictable when generators work in a networked form Vaidya et al. (1999). The frequency correction in a network with synchronous machines implies the use of a large quantity of energy in a short time. Therefore, the problem of reducing the control effort by determining the optimal control signal is of relevant importance. Model predictive control (MPC) is an alternative to overcome the limitations of classical controllers, allowing the inclusion of particular restrictions. MPC might use directly the nonlinear model of the improved swing equation; however, the nonlinear nature and the restrictions inherent to the problem can be problematic to solve it on a finite horizon.

The Koopman operator allows to describe a dynamical system as a linear one but of infinite dimension in a new space known as the space of observables Budišić et al. (2012). This representation is highly convenient for MPC design, simplifying the optimization process by changing the nonlinear model for a linear one in the space of observables or lifted-space. The Koopman representation can be determined by several algorithms; in particular, data-based methods offer a considerable advantage due to the availability of measurement from real sources or detailed simulations. Among some of the data-based methods are the dynamic mode decomposition (DMD) Tu et al. (2014), and extended dynamic mode decomposition (EDMD) Williams et al. (2015). The last one uses a dictionary of functions or bases to lift the set of measure-

10.1016/j.ifacol.2022.07.242

ments from the system and the least-squares minimization method to get a matrix representation of the Koopman operator. Several works have used the Koopman operator in power systems defined by the swing equation. Korda et al. (2018) uses EDMD to build a linear representation of a set of generators described by the swing equation. There, a centralized approach is used to control the set of machines. A Koopman model to enhance the transient stability of a power grid defined by the swing equation is presented by Ping et al. (2021), the Koopman model is improved by using neural networks to learn the basis function in the EDMD algorithm; also they used a centralized approach to improve the stability. King et al. (2021) uses the EDMD algorithm to get a linear model of the power system; it is used to solve an economic dispatch problem.

The main objective of this paper is to present a distributed MPC control using a Koopman data-based approximation of a network of synchronous machines based on the improved swing equation. The Koopman representation is obtained using EDMD to construct a linear predictor for distributed model predictive control (DMPC). The DMPC is presented in two perspectives: non-cooperative and a cooperative; both approaches are compared with the decentralized one presented by Korda et al. (2018).

The rest of the paper is organized as follows: Section 2 presents the improved swing equation, and the form of finding the Koopman operator using the EDMD algorithm. In Section 3, it is shown the linear predictor design based on the Koopman operator, and the distributed MPC control design with a non-cooperative and cooperative approach. Section 4 shows a case study for a networked system simulated in Matlab for three scenarios. Finally, conclusions are presented in Section 5.

Notation Throughout this paper, $||\cdot||_Q^2$ denotes the product between the Euclidean norm of $\cdot$ and matrix Q. $\mathcal{L}$ denotes the Laplacian matrix, Y the admittance matrix, and $\mathcal{N}_i$ denotes the set of neighbors of the i^{th} agent.

2. IMPROVED SWING EQUATION AND KOOPMAN OPERATOR

In this Section, it is shown the improved swing equation, and after the generalities of the Koopman operator and EDMD algorithm.

2.1 Improved swing equation

The improved swing equation is presented by Zhou and Ohsawa (2008); the angular frequency ω_0 is used to determine the rotor angular displacement θ by a fixed reference axis fixed at an infinite bus. The displacement is given as $\theta = \omega_0 t + \delta, \quad t > t_0$, where t_0 is the initial time, and δ is the rotor angular displacement regarding the synchronous reference axis.

The mathematical model in per unit for a network with N interconnected synchronous generators, including the impedance between lines, is given by the nonlinear swing equation Ping et al. (2021) of the form

$$\begin{aligned} \frac{d\delta_i}{dt} &= \omega_i - \omega_s \\ \frac{2H_i}{\omega_s}\frac{d\omega_i}{dt} + \frac{D_i}{\omega_s}\omega_i &= P_{m,i} - \sum_{j=1}^{N} |E_i E_j| B_{ij} \sin(\delta_i - \delta_j) \\ &\quad - \sum_{j=1}^{N} |E_i E_j| G_{ij} \cos(\delta_i - \delta_j) - E_i^2 G_{ii} P_{m,i} + u_i, \end{aligned} \tag{1}$$

where H_i represents the inertia, D_i is the damping constant, ω_s is the frequency of reference, δ_i is the rotor angle, $P_{m,i}$ is the mechanical power input, E_i is the voltage measured at the i^{th} generator, u_i is the control input, the matrix of admittance between generators is given by Y, whose elements are given by $Y_{id} = G_{id} + jB_{id}$, and G_{ii} is the self-conductance.

2.2 Koopman operator and EDMD

Consider a nonlinear discrete-time dynamical system defined by

$$x_{k+1} = f(x_k) \tag{2}$$

that represents the dynamics of the synchronous generator, with $f : \mathcal{M} \to \mathcal{M}$ being the space of evolution of the system.

The Koopman operator is a linear but infinite dimensional operator $\mathcal{K} : \mathcal{F} \to \mathcal{F}$ where $\mathcal{F}$ is an invariant subspace spanned by a set of observables $\psi \in \mathcal{F}$, and $\psi : \mathcal{M} \to \mathbb{C}$.

The composition operator is given by

$$\mathcal{K}\psi(x_k) = \psi(f(x_k)) = \psi(x_{k+1}), \tag{3}$$

and maps the value of the observable function one step further. As the Koopman operator is linear, a set of eigenfunctions and eigenvalues is defined

$$\mathcal{K}\varphi_l = \lambda_l \varphi_l(x_k) \tag{4}$$

where φ_l are the eigenfunctions corresponding to the observable function, and λ_l are the corresponding eigenvalues of $\mathcal{K}$.

The observable function ψ can be written as

$$\psi(x_{k+1}) = \mathcal{K}\psi(x_1) = \sum_{l=1}^{\infty} \lambda_l \varphi_l(x_1) v_l \tag{5}$$

where v_l is known as the Koopman mode. Instead of calculating the infinite sum of (5), ψ can be approximated by a data-based technique, such as DMD and its extension EDMD.

EDMD is a data-driven technique based on DMD. First, a set of N_k observables is defined

$$\mathcal{D} = \{\psi_1 \quad \psi_2 \quad \dots \quad \psi_{Nk}\}.$$

From a dynamic system given by $y_i = F(x_i)$, two sets of data are generated as

$$X = [x_1 \quad x_2 \quad \dots \quad x_M], \qquad Y = [y_1 \quad y_2 \quad \dots \quad y_M]$$

where Y is a shifted version of X.

Then, it is defined the vector value function

$$\Psi(x) = [\psi_1(x) \quad \psi_2(x) \quad \dots \quad \psi_{Nk}(x)].$$

Two square matrices are defined as follows:

$$G = \frac{1}{M}\sum_{m=1}^{M} \Psi(x_m)^* \Psi(x_m)$$

$$A = \frac{1}{M}\sum_{m=1}^{M} \Psi(x_m)^* \Psi(y_m)$$

where, * denotes the transpose, then the Koopman matrix K is calculated by

$$K = G^{\dagger} A$$

where † denotes the pseudo-inverse.

In the next section, the EDMD algorithm is used to generate a linear predictor of the networked synchronous generator system, and the distributed MPC approaches are presented.

3. LIFTED SPACE DESIGN AND DISTRIBUTED MPC

This section presents the design of a linear predictor for the networked generators system. Then, it is shown the design of the distributed model predictive control to regulate the frequency of the system.

3.1 Linear Predictor and Distributed Model Predictive Control

Linear predictors for nonlinear systems are designed by using the Koopman representation of the system Mauroy et al. (2020). For a Koopman matrix A with N_k eigenvalues of the form $\lambda_1, \ldots, \lambda_{Nk}$, and a vector of observables ϕ, the next linear predictor is defined

$$\begin{aligned} \dot{z} &= Az + Bu \\ z_0 &= \phi(x_0) \\ y &= Cz \end{aligned} \tag{6}$$

where

$$A = \begin{bmatrix} \lambda_1 & & \\ & \ddots & \\ & & \lambda_{Nk} \end{bmatrix} \qquad \phi = \begin{bmatrix} \phi_1 \\ \vdots \\ \phi_{Nk} \end{bmatrix}$$

The dynamic of each generator is represented by selecting the set of functions or dictionary to find the Koopman operator. However, the coupling between generators implies that changes over one generator affect the dynamics of the whole interconnected system. Several approaches to deal with coupling have been proposed, among them the non-cooperative and the cooperative control Stewart et al. (2010).

A general schematic for distributed MPC control is shown in Fig. 1. The optimization process depends on the linear representation of each system, and the Laplacian matrix representing the connections among generators.

3.2 Non-cooperative distributed MPC

This approach includes a matrix for the consensus among the frequency values coming from each agent $\mathcal{L}_{ij}$, the cost functions are the same as the decentralized approach and are local. The non-cooperative distributed control based on the linear predictor defined in (6) is defined as follows

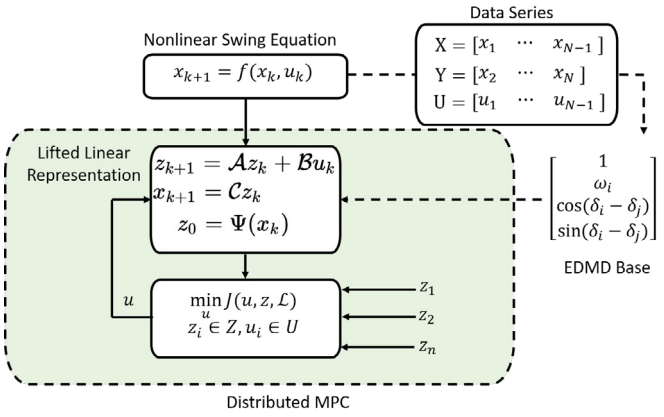

Fig. 1. Linear Koopman Predictor

$$\min_{u^i} V_i = \min_{u^i} \sum_{k=0}^{H_p-1} ||\omega_k^i - \omega_k^{ref,i}||_Q^2 + ||u_k^i||_R^2 \tag{7}$$

$$\text{s.t} \quad \omega_{k+1}^i = \mathcal{A}_i \omega_k^i + \mathcal{B}_i u_k^i + \sum_{j \in \mathcal{N}_i} \mathcal{L}_{ij} \hat{\omega}_k \tag{8}$$

where H_p is the prediction horizon, the vector with the values from the neighbors is $\hat{\omega} = [\omega_1 \quad \ldots \quad \omega_i \quad \omega_N]^\top$, and Q and R are the constants for the error and control actions, respectively.

3.3 Cooperative distributed MPC

This approach includes the coupling between agents given by the consensus between states represented by the Laplacian matrix $\mathcal{L}$. There is a global cost function V given by the weighted sum of the local cost functions V_i coming from the set of neighbors of the i^{th} agent Chen et al. (2020). The global cost is given by

$$V = \sum_{i \in \mathcal{N}_i}^{N} \rho_i V_i = \sum_{k=0}^{H_p-1} ||\omega_k - \omega_k^{ref}||_Q^2 + ||u_k||_R^2 \tag{9}$$

$$\text{s.t} \quad \omega_{k+1}^i = \omega_k^i + \mathcal{A}_i \omega_k^i + \mathcal{B}_i u_k + \sum_{j \in \mathcal{N}_i} \mathcal{L}_{ij} \hat{\omega}_k \tag{10}$$

where $\hat{\omega} = [\omega_1 \quad \ldots \quad \omega_i \quad \omega_N]^\top$, ρ_i is the weight factor for the i^{th} cost function, and $u = [u_1 \quad \ldots \quad u_i \quad u_N]^\top$.

3.4 Function Selection for the Koopman Representation

The approximated Koopman representation of the networked system is calculated using the dictionary or base functions used in Mauroy et al. (2020), which is a more specific case of the bases used in Korda and Mezic (2020). The constant value, the frequency, and the sin and cos functions of the phase differences between generators are used as base functions. For the networked system with N synchronous generators, the vector of observers for the i^{th} generator is defined as

$$\psi_i = [1 \quad \omega_i \quad \cos(\delta_i - \delta_j) \quad \sin(\delta_i - \delta_j)], \tag{11}$$

where $i = 1, \ldots, N$ with $i \neq j$. Thus, we can find a Koopman representation for each generator that also depends on the connection between them. The simulations to

generate the trajectories and collect the data are presented in the next Section.

4. CASE OF STUDY

In this section, a five-generator interconnected system in a per unit model, as it is shown in Fig. 2 is simulated. The parameters of the system are presented in TABLE 1, the Laplacian matrix L that defines the connections among generators is given by

$$L = \begin{bmatrix} 1 & -1 & 0 & 0 & 0 \\ -1 & 2 & -1 & 0 & 0 \\ 0 & -1 & 3 & -1 & -1 \\ 0 & 0 & -1 & 1 & 0 \\ 0 & 0 & -1 & 0 & 1 \end{bmatrix}$$

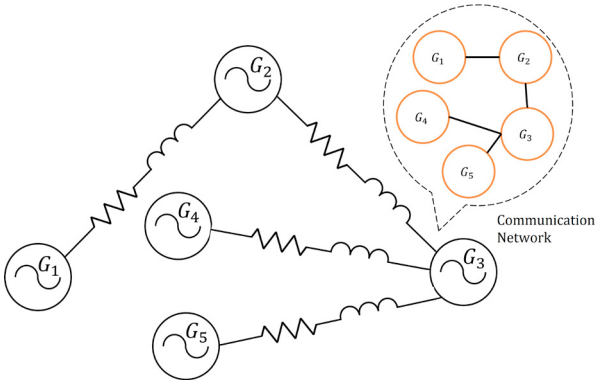

Fig. 2. Network of SGs

Table 1. Generator's Parameters

Parameter	H	D	ω	E
SG_1	0.10	0.80	1	1.00
SG_2	0.20	0.70	1	1.00
SG_3	0.30	0.60	1	1.00
SG_4	0.35	0.65	1	1.00
SG_5	0.40	0.69	1	1.00
Frequency	60Hz - 1.0 p.u			
Line Yij	$Y_{12} = 0.0142 - 0.3765i$ $G_{11} = 10$			
	$Y_{23} = 0.4531 - 0.6009i$ $G_{22} = 10$			
	$Y_{34} = 0.3641 - 0.5019i$ $G_{22} = 10$			
	$Y_{35} = 0.1271 - 0.2849i$ $G_{22} = 10$			

4.1 Koopman and EDMD Simulations

Based on (1), a discretized model using Euler is simulated in Simulink to generate the data to find the Koopman representation and the set to verify the Koopman approximation for each generator. Measurements of the phase and angular frequency from each generator are collected with a sample time $T_s = 0.1$s, varying the initial condition for frequency $\omega(0)$ each 10s; also the mechanical power and the voltage values vary each 23s. The mechanical power is selected to be used as a control input. The total time of simulation is 1000s; collecting a series of data $M = 10000$ and 1000 samples to verify the Koopman approximation

The results for the Koopman approximations of (1) are shown in Fig. 3. The approximation is better at the beginning and starts to be badder when time passes. However, for the use of MPC, we are interested in a short time.

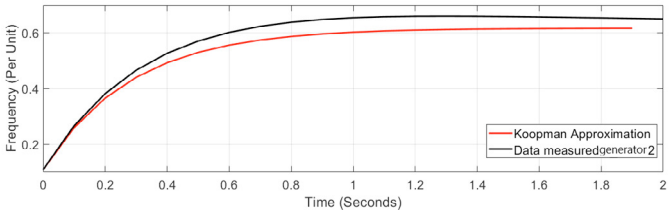

Fig. 3. Koopman representation and values measurement at generator two

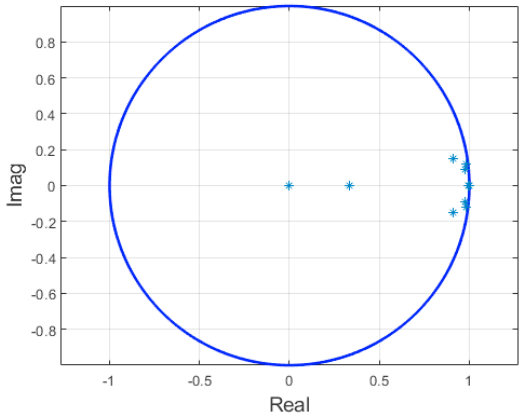

Fig. 4. Eigenvalues of Koopman Matrix for generator one

It is also possible to determine the set of eigenvalues of A_1 for the set of 16-based functions, which is plotted in the unit circle as shown in Fig. 4. Most of the eigenvalues are close together and around $(0, 1)$. This is very practical for dimension reduction of the system. In this case, eigenvalues close to zero can be omitted.

4.2 Decentralized and Distributed MPC Simulations

In this section it is shown the performance of the proposed algorithms. The five generators are interconnected through transmission lines. The predictive control performance is evaluated first for frequency regulation and then for voltage changes. The parameters for the interconnected system are shown in Table 2.

Table 2. MPC Parameters.

Paremeter	Generator 1 to 5
State difference gain Q	100
Input gain R	1
Consensus gain α	0.1
Sampling Time	Ts=0.1s
Frequency restriction	$0.9 \leq \omega_i \leq 1.1$
Control Horizon H_p	10
Wight factor ρ_i	$\rho_1 = 0.8, \quad \rho_2 = 0.1, \quad \rho_3 = 0.1$

4.2.0.1. Decentralized MPC This part partially reproduces the results presented by Mauroy et al. (2020), and Korda et al. (2018). Each generator has a predictive controller and there is no communication among agents. Three generators connected through transmission lines as shown in Fig. 2. The power system starts working without control at $t = 0$s and the predictive control for each generator is activated at $t = 5$s.

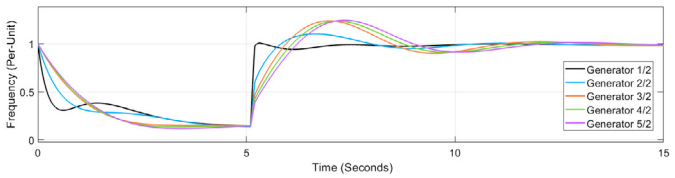

Fig. 5. Per-unit frequency before and after active the predictive control signal at $t = 5$s with decentralized approach.

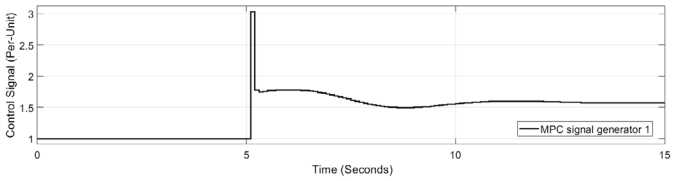

Fig. 6. MPC signal applied to generator one after $t = 5$s

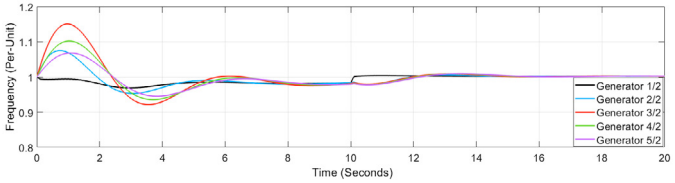

Fig. 7. Frequency response after an abrupt voltage change in generator one at $t = 10$s.

The frequency reaches the reference value in finite time as shown in Fig. 5, and the control signal is shown in Fig. 6. The performance of the predictive controller to disturbances is checked by changing the voltage of the generator one at $t = 10$s, the voltage drops from $E = 1.0$ to $E = 0.9$. The frequency response is shown in Fig. 7 reaching the reference value after several seconds.

4.2.0.2. Non-Cooperative Distributed Approach Simulations The interconnected generators are controlled by a non-cooperative distributed predictive control. The communication graph used to check the performance of the system is shown in Fig. 2.

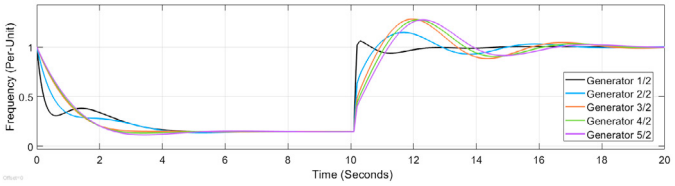

Fig. 8. Frequency response of the system before and after the noncooperative control is activated at $t = 10$s.

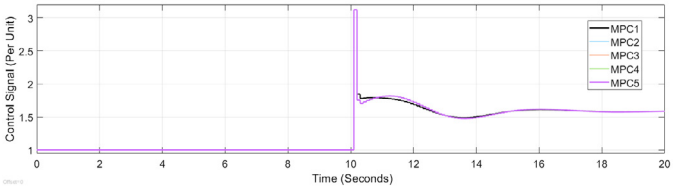

Fig. 9. Noncooperative control signal activated at $t = 10$s.

The non-cooperative distributed control is activated at $t = 10$s, then the system achieves the frequency of reference as shown in Fig. 8. The control signal for each generator is shown in Fig. 9 reaching consensus after some seconds.

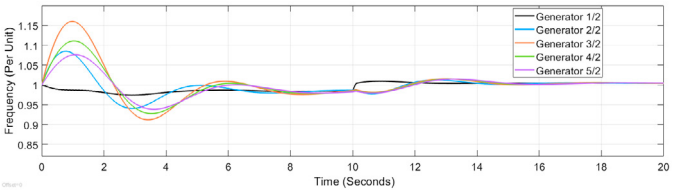

Fig. 10. Frequency response of the noncooperative approach when the voltage at generator one falls from 1 to 0.9 p.u at $t = 10$s.

Same as for the centralized approach, the voltage of generator one drops at $t = 10$s. The frequency response is shown in Fig. 10. After the disturbance at $t = 10$s, the frequency gets close to the reference value; however, it lays in a window with an error inferior to 1%.

4.2.0.3. Cooperative Distributed Approach Simulations The interconnected generators are controlled by a cooperative distributed predictive control using the graph shown in Fig. 2 with weight factors ρ_i as shown in Table 2.

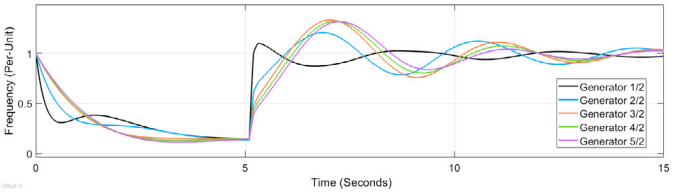

Fig. 11. Per-unit frequency before and after active the predictive control signal at $t = 5$s with a cooperative distributed approach.

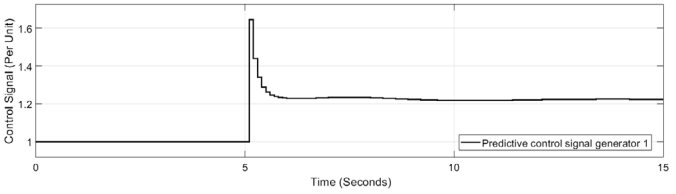

Fig. 12. MPC signal applied to generator one after $t = 5$s

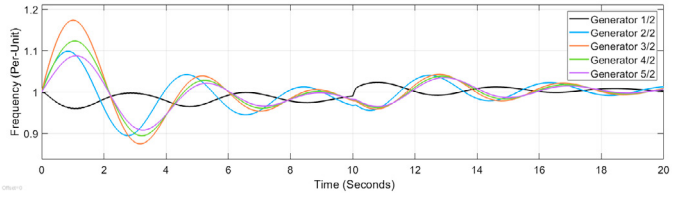

Fig. 13. Frequency response after an abrupt voltage change in generator one at $t = 10$s.

The cooperative distributed control is activated at $t = 5$s, then the system achieves the frequency of reference as shown in Fig. 11. The control signal for the first generator is shown in Fig. 12. A fault is also simulated when the voltage at generator one drops from $E = 1$ to $E = 0.9$

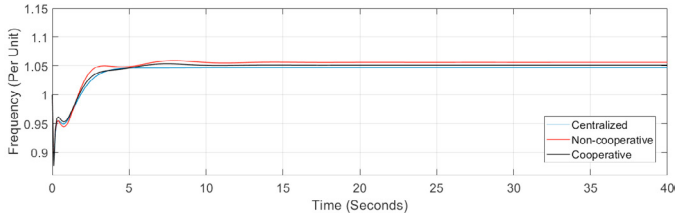

Fig. 14. Frequency response for the first generator using the three control approaches

at $t = 10$s, the frequency of each generator is shown in Fig. 13.

The frequency response for each control approach is shown in Fig. 14. The controllers function since $t = 0$s achieving a value close to the reference with an error inferior to one percent.

5. CONCLUSION

An interconnected system of synchronous generators is modeled by the nonlinear swing equation, and it is represented by a linear predictor in the space of observables by means of the Koopman operator. The frequency of the interconnected system is controlled using model predictive control in a distributed way following a non-cooperative, and a cooperative approach. It is shown that the cooperative approach reaches the reference value in a finite time while keeping the restrictions; however, it is more complex and computational time consuming. As a future work, it is interesting to used the linear representation with a distributed optimization algorithm such as Alternate Direction Multipliers Method (ADMM).

REFERENCES

Bouzid, A.M., Guerrero, J.M., Cheriti, A., Bouhamida, M., Sicard, P., and Benghanem, M. (2015). A survey on control of electric power distributed generation systems for microgrid applications. *Renewable and Sustainable Energy Reviews*, 44, 751–766. doi: 10.1016/j.rser.2015.01.016.

Budišić, M., Mohr, R., and Mezić, I. (2012). Applied Koopmanism. *Chaos*, 22(4). doi:10.1063/1.4772195.

Caliskan, S.Y. and Tabuada, P. (2015). Uses and abuses of the swing equation model. In *2015 54th IEEE Conference on Decision and Control (CDC)*, 6662–6667. doi:10.1109/CDC.2015.7403268.

Chen, M., Zhao, J., Xu, Z., Liu, Y., Zhu, Y., and Shao, Z. (2020). Cooperative distributed model predictive control based on topological hierarchy decomposition. *Control Engineering Practice*, 103(April), 104578. doi: 10.1016/j.conengprac.2020.104578.

Kaiser, E., Kutz, J.N., and Brunton, S. (2021). Data-driven discovery of Koopman eigenfunctions for control. *Machine Learning: Science and Technology*, 98195, 1–40. doi:10.1088/2632-2153/abf0f5.

King, E., Bakker, C., Bhattacharya, A., Chatterjee, S., Pan, F., Oster, M.R., and Perkins, C.J. (2021). Solving the Dynamics-Aware Economic Dispatch Problem with the Koopman Operator. *e-Energy 2021 - Proceedings of the 2021 12th ACM International Conference on Future Energy Systems*, 137–147. doi: 10.1145/3447555.3464864.

Korda, M. and Mezic, I. (2020). Optimal Construction of Koopman Eigenfunctions for Prediction and Control. *IEEE Transactions on Automatic Control*, 65(12), 5114–5129. doi:10.1109/TAC.2020.2978039.

Korda, M., Susuki, Y., and Mezić, I. (2018). Power grid transient stabilization using Koopman model predictive control. *IFAC-PapersOnLine*, 51(28), 297–302. doi: 10.1016/j.ifacol.2018.11.718.

Mauroy, A., Susuki, Y., and Mezić, I. (2020). *Introduction to the koopman operator in dynamical systems and control theory*, volume 484. doi:10.1007/978 – 3 – 030 – 35713 – 9_1.

Monshizadeh, P., De Persis, C., Monshizadeh, N., and van der Schaft, A.J. (2016). Nonlinear analysis of an improved swing equation. In *2016 IEEE 55th Conference on Decision and Control (CDC)*, 4116–4121. doi: 10.1109/CDC.2016.7798893.

Ping, Z., Yin, Z., Li, X., Liu, Y., and Yang, T. (2021). Deep Koopman model predictive control for enhancing transient stability in power grids. *International Journal of Robust and Nonlinear Control*, 31(6), 1964–1978. doi: 10.1002/rnc.5043.

Stewart, B.T., Venkat, A.N., Rawlings, J.B., Wright, S.J., and Pannocchia, G. (2010). Cooperative distributed model predictive control. *Systems and Control Letters*, 59(8), 460–469. doi:10.1016/j.sysconle.2010.06.005.

Tamrakar, U., Copp, D., Nguyen, T.A., Hansen, T.M., and Tonkoski, R. (2020). Optimization-based fast-frequency estimation and control of low-inertia microgrids. *IEEE Transactions on Energy Conversion*.

Tu, J.H., Rowley, C.W., Luchtenburg, D.M., Brunton, S.L., and Kutz, J.N. (2014). On dynamic mode decomposition: Theory and applications. *Journal of Computational Dynamics*, 1(2), 391–421. doi: 10.3934/jcd.2014.1.391.

Vaidya, U., Banavar, R., and Singh, N. (1999). A chaotic phenomenon in the damped power swing equation. In *Proceedings of the 38th IEEE Conference on Decision and Control (Cat. No.99CH36304)*, volume 5, 4650–4655 vol.5. doi:10.1109/CDC.1999.833276.

Williams, M.O., Kevrekidis, I.G., and Rowley, C.W. (2015). A Data–Driven Approximation of the Koopman Operator: Extending Dynamic Mode Decomposition. *Journal of Nonlinear Science*, 25(6), 1307–1346. doi: 10.1007/s00332-015-9258-5.

Zhou, J. and Ohsawa, Y. (2008). Improved swing equation and its properties in synchronous generators. *IEEE Transactions on Circuits and Systems I: Regular Papers*, 56(1), 200–209.